

Histomorphometric characterization of the endometrium in mules (*Equus mulus*): An approach to endometritis/endometrosis

Miguel A. Gutiérrez-Reinoso ^{a,b,c}, Pedro M. Aponte ^{d,e}, Manuel García-Herreros ^{f,g,✉}, Katlhen G. García-Bravo ^b, Daniela Rojas ^{h,✉}, Yat Sen Wong ^c, Fernando Saravia ^c, Fidel Ovidio Castro ^{c,✉}, Jaime Catalán ^{i,j,1,*}, Jordi Miró ^{a,1,✉*}

^a Equine Reproduction Service, Department of Animal Medicine and Surgery, Faculty of Veterinary Sciences, Autonomous University of Barcelona, Cerdanya de la Vallès ES-08193, Spain

^b Carrera de Medicina Veterinaria, Facultad de Ciencias Agropecuarias y Recursos Naturales, Universidad Técnica de Cotopaxi, (UTC), Latacunga 050150, Ecuador

^c Department of Animal Science, Faculty of Veterinary Sciences, Universidad de Concepción, Chillán 3780000, Chile

^d Colegio de Ciencias Biológicas y Ambientales (COCIBA), Universidad San Francisco de Quito (USFQ), Quito 170901, Ecuador

^e Instituto de Investigaciones en Biomedicina "One-Health", Universidad San Francisco de Quito (USFQ), Campus Cumbayá, Quito 170901, Ecuador

^f National Institute for Agricultural and Veterinary Research (INIAV), Santarém 2005-424, Portugal

^g CIISA-AL4AnimalS, Faculty of Veterinary Medicine, University of Lisbon (UL), Lisbon 1300-477, Portugal

^h Department of Pathology, Faculty of Veterinary Sciences, Universidad de Concepción, Chillán 3780000, Chile

ⁱ Biotechnology of Animal and Human Reproduction (TechnoSperm), Institute of Food and Agricultural Technology, University of Girona, Girona ES-17003, Spain

^j Unit of Cell Biology, Department of Biology, Faculty of Sciences, University of Girona, Girona ES-17003, Spain

ARTICLE INFO

Keywords:

Mulke
Biopsy
Histological characterization
Proinflammatory genes
Degenerative endometrial fibrosis

ABSTRACT

Mules (*Equus mulus*), as sterile hybrids between mares and donkeys, present a unique uterine morphology and physiology that remains poorly characterized. This study provides the first histomorphometric evaluation and transcriptional profiling of the endometrium in adult mules. To achieve this, endometrial biopsies were analysed using quantitative stereology, histological classification (Kenney-Doig system), and qPCR of key immune-related and fibrotic genes. Histometric analyses revealed that the stratum spongiosum was the predominant component of the mule endometrium (mean volume density: 84.7 %), whereas the epithelium and compact layers accounted for smaller proportions. This distribution, more pronounced than what is typically reported in mares, suggests enhanced stromal expansion or edema. Endometrial glands were abundant, and the overall structural profile exhibited an intermediate phenotype with a clear asinine bias. Most samples were classified as grades I, IIA, or IIB, with no specimens reaching grade III. Mild to moderate stromal remodeling, preserved tissue architecture, and inflammatory signatures –characterized by increased relative abundance of IL1B, IL6, and TNF α transcripts– were observed in higher grades and were consistent with early stages of endometrial degeneration. Although these features indicate early degenerative changes, the hybrid reproductive physiology of mules, including limited hormonal cyclicity, may contribute to reduced progression

* Corresponding author at: Biotechnology of Animal and Human Reproduction (TechnoSperm), Institute of Food and Agricultural Technology, University of Girona, Girona ES-17003, Spain.

** Corresponding author.

E-mail addresses: jaime.catalan@udg.edu (J. Catalán), jordi.miro@uab.cat (J. Miró).

¹ Joint senior authors.

towards fibrosis. This integrated histological–molecular assessment reinforces the diagnostic value of the Kenney–Doig system in mules and supports the adaptation of a refined IIC grade to better capture hybrid-specific features. Overall, the mule endometrium displays distinct yet comparable traits relative to that of horses and donkeys, highlighting its potential as a comparative model for equine reproductive research. These findings provide a foundation for improved clinical decision-making and future studies on hybrid fertility and uterine health.

1. Introduction

The mule, a sterile hybrid resulting from the cross between a mare (*Equus caballus*) and a donkey (*Equus asinus*), has traditionally been valued for its endurance and work capacity in equestrian, agricultural, and military activities (Davis, 2019). Although generally considered infertile, there are reports of successful pregnancies (Rong et al., 1985, 1988; Ryder et al., 1985; Henry et al., 1995), suggesting that mules' reproductive physiology may present unique characteristics (Canisso et al., 2019). This biological singularity has attracted growing scientific interest, within reproductive biotechnology, where the ability of mules to carry pregnancies to term via embryo transfer has been documented (Allen and Short, 1997; González et al., 2015; Bottrel et al., 2017; Camargo et al., 2020; Fanelli et al., 2022). Together, these findings highlight the relevance of the mule as a model for studying uterine function in the context of interspecific gestation.

The endometrium, critical for reproductive efficiency through its role in embryo implantation, has been extensively characterized in mares (Klein, 2015), particularly through the histological classification proposed by Kenney and Doig (1986), which allows correlation of structural changes with fertility (Kenney and Doig, 1986; Herrera et al., 2018; Schöniger and Schoon, 2020). Likewise, the expression of molecular markers related to inflammation and tissue remodeling has been described in pathologies such as endometritis and endometrosis (Woodward and Troedsson, 2015; Elshalofy et al., 2022; Ulaangerel et al., 2025). Similar studies have also been conducted in jennies, although in a more limited scope (Miró et al., 2020; Radar-Chafirovitch et al., 2025).

While the endometrial architecture is broadly conserved among equids, each species exhibits distinct histological features that reflect functional adaptations. The donkey endometrium is anatomically similar to that of the mare in terms of layers, presenting the same basic compartments: luminal epithelium, endometrial stroma (compactum and spongiosum), endometrial glands, and underlying vascular and lymphatic vasculature. However, species-specific traits influence both physiology and pathology, including variations in immune cell distribution, basal inflammatory infiltrate, presence of eosinophils, and fibrosis patterns, which may differ from horses. In mares, endometrial alterations such as periglandular fibrosis, glandular nesting, and the progressive replacement of collagen type III by collagen type I have been well documented and correlated with decreased fertility (Miró et al., 2020). In contrast, donkeys exhibit a distinctive pattern in collagen distribution, with type III collagen persisting in the compact layer even at advanced stages of degenerative endometrial fibrosis, while simultaneously type I collagen increases in the deeper stroma and periglandular regions. In terms of immune infiltration, the scarce presence of eosinophils in mares contrasts with the prominent eosinophilic infiltration observed in the endometrium of donkeys, where it serves as a notable histological marker (Miró et al., 2020). Donkeys exhibit a relatively stable population of resident immune cells, particularly T lymphocytes, across varying stages of degenerative endometrial fibrosis, which may indicate a distinctive pattern of uterine immune regulation (Radar-Chafirovitch et al., 2025). The mule, a sterile hybrid, remains relatively understudied in scientific literature. However, preliminary evidence indicates that its endometrial structure may resemble that of the donkey more than that of the mare (Canisso et al., 2019). These observations suggest that while mules share the fundamental structural organization of the equine endometrium, their histological phenotype may be preferentially aligned with asine traits, underscoring the need for dedicated studies to confirm whether hybridization produces unique uterine patterns of uterine remodeling.

Despite this progress in mares and donkeys, the mule endometrium remains virtually unexplored (Allen, 2005; Gambini et al., 2025). To date, no published studies have detailed the histological structure or molecular marker expression in mule (*Equus mulus*). This knowledge gap is particularly relevant given the hybrid nature of the species, which may give rise to specific endometrial characteristics not fully predictable from either parent species. Studies on hybrids of other species have shown that hybridization can induce specific tissue and molecular alterations (Gabryś et al., 2021; Adavoudi and Pilot, 2022; Runemark et al., 2024), which further supports the need to study the mule endometrium using modern analytical tools.

On the other hand, to date, no studies have provided an integrated histological and molecular characterization of the mule endometrium. Comprehensive analysis combining conventional histological techniques, unbiased stereology, and messenger RNA (mRNA) transcripts analysis of genes associated with inflammation (IL-1 β , IL-6, TGF- β , and TNF- α) are previously validated in mares (Szóstek-Mioduchowska et al., 2019; Lection et al., 2024). This integrative methodology enables a robust, quantitative, and biologically meaningful evaluation of both tissue structure and functional molecular status.

The objective of this study was to characterize the histological architecture and expression of key inflammatory mediators in the mule endometrium, with an emphasis on morphometric parameters and immune-related mRNA transcripts abundance. Defining the endometrial phenotype of the mule will provide a comparative framework relative to mares and donkeys, enhance diagnostic precision, refine the clinical management of endometrial disorders in equids, and contribute to the development of reproductive biotechnologies tailored to hybrid species.

2. Materials and methods

2.1. Ethics statement

The authors certify that this study was conducted in strict accordance with ethical principles for animal research, following the international ARRIVE guidelines (Animal Research: Reporting of In Vivo Experiments), available at <http://www.nc3rs.org.uk/ARRIVEchecklist> (accessed July 7, 2023). The experimental protocol was reviewed and approved by the Bioethics Committee for the Use of Experimental Animals at Universidad de Concepción, Chillán Campus, Chile, under approval number CBE-8269/2023, dated September 1, 2023.

As this study was conducted exclusively with animals managed under institutional care, informed consent from individual owners was not required. All mules used in this research belonged to the Riñihue Military Breeding Center, which formally authorized the use of the animals for scientific purposes under veterinary supervision and in compliance with the procedures approved by the Bioethics Committee of Universidad de Concepción (Approval Code: CBE-8269/2023). Throughout the study, animal welfare was strictly monitored, and all procedures were carried out by trained personnel to ensure humane handling and minimize stress, in accordance with current national and international regulations on animal experimentation.

2.2. Animals and biopsies

Endometrial samples were obtained from 22 mules, aged between five and ten years, all of which were in estrus at the time of sampling. The animals were housed at the Riñihue Military Breeding Center, located in the commune of Los Lagos, Valdivia Province, Los Ríos Region, Chile.

None of the mules had previously participated in reproductive programs, such as embryo recipient protocols, and had no history of pregnancy or parturition. Selection criteria included reproductive age, physiological status, and absence of clinical history of uterine pathology. Each animal underwent a gynecological examination using vaginoscopy and transrectal ultrasonography with a SonoScape X3Vet® system (SonoScape Medical Corp, Shenzhen, Guangdong, China) equipped with a 5.0 MHz linear transducer. This procedure confirmed estrus and ruled out anatomical or functional abnormalities of the reproductive tract. The mules included in the study showed a preovulatory follicle diameter higher than 35 mm, absence of corpus luteum and endometrial edema. Non-cycling females were excluded from the study. Endometrial biopsy samples were obtained from adult female mules using a standard transrectal approach, following established veterinary protocols for equine endometrial sampling. Before the procedure, animals were gently restrained in a padded chute to minimize movement and reduce stress. The perineal area was thoroughly cleaned with a povidone-iodine solution and subsequently rinsed with sterile saline to minimize the risk of contamination.

To collect the sample, a sterile equine endometrial alligator-type biopsy forceps was introduced transvaginally, while a lubricated, gloved hand was inserted into the rectum to stabilize the uterus. The forceps were then guided through the cervix into the uterine body under rectal palpation. A single tissue sample ($\sim 0.5\text{--}1.0\text{ cm}^3$) was carefully collected from the beginning of a uterine horn. After retrieval, the collected sample was divided into two portions. One was immediately placed in 4 % formaldehyde for histological analysis, while the other was immersed in RNAlater® solution (Invitrogen, Thermo Fisher Scientific, Waltham, MA, USA) for RNA stabilization and subsequent molecular analysis.

2.3. Histology

Tissue fixation in 4 % formaldehyde was carried out for 24 h. After fixation, samples were transferred to 70 % ethanol and stored at 4 °C until histological processing at the Instituto de Biodiversidad Tropical (IBIOTROP), Laboratorio de Salud Animal, Universidad San Francisco de Quito (USFQ), Quito, Ecuador. Unless noted otherwise, all reagents used in the procedures were provided by Sigma-Aldrich® (Merck KGaA, St.Louis, MO, USA).

Tissue samples underwent standard histological processing, which included sequential dehydration steps in 70 % ethanol ($2 \times 1\text{ h}$), 95 % ethanol (1 h), and absolute ethanol ($3 \times 20\text{ min}$), followed by clearing in xylene ($3 \times 5\text{ min}$). The samples were then embedded in paraffin using a progressive protocol: xylene: paraffin mixtures (1:1 and 1:2) and finally pure paraffin at 58 °C ($2 \times 1\text{ h}$). Sections were cut at a thickness of 4 μm using a Leica RM2125 RTS microtome (Leica Microsystems GmbH, Wetzlar, Germany).

Sections were stained with Harris hematoxylin. The protocol included clearing in xylene ($3 \times 3\text{ min}$), rehydration through graded ethanol (100 % and 95 %, $2 \times 1\text{ min}$ each), rinsing in distilled water ($2 \times 3\text{ min}$), and staining with Harris hematoxylin for 15 s, followed by a 10-minute wash under running tap water. Sections were dehydrated using 95 % and 100 % ethanol ($2 \times 1\text{ min}$ each), followed by clearing in xylene ($3 \times 1\text{ min}$). Finally, the slides were mounted using SecureMount™ (Thermo Fisher Scientific, Waltham, MA, USA) in preparation for morphometric and stereological analysis.

2.4. Stereology

Images were captured using the digital capturing system Labscope, Zeiss (Leica Microsystems GmbH, Wetzlar, Germany) coupled to a light microscope Zeiss PrimoStar 3 (Leica mycosystems GmbH, Wetzlar, Germany) at a total magnification of $20 \times$. Cross-sectional diameters or heights of the structures were measured directly from the digital images using ImageJ software (downloaded from <https://imagej.net/ij/>), with an average of 25 measurements per endometrial sample per animal in 22 mules.

Endometrial volume densities were estimated using a digital grid image (point test system) consisting of 48 points (8×6) randomly

placed as a transparent layer over the captured endometrial digital images with the software Adobe Photoshop (version 21.0.3). The number of points landing on the different endometrial compartments (Epithelium, Compact Layer, Spongy Layer, Glands, Lymphatic Vessels, Capillaries) was recorded for volume density estimation using the formula $V_V = P_p/P_T$, where P_p represents the number of points landing on a specific compartment or phase and P_T represents the total number of points landing on the reference space (endometrial image). Data were derived from 550 individual observations, subjected to statistical refinement, and provide a systematic histomorphological characterization of endometrial tissue in this hybrid species.

2.5. Histopathological analysis of the endometrium

Endometrial alterations were classified according to the Kenney and Doig classification (Kenney and Doig, 1986), which grades the tissue as I, IIA, IIB, or III based on glandular degeneration, periglandular fibrosis, chronic inflammatory infiltrate, and other indicators of reproductive function.

2.6. RNA extraction and cDNA synthesis

Mules' endometrial biopsies preserved in RNAlater® medium (Invitrogen, Thermo Fisher, Waltham, MA, USA.) were used for RNA extraction and cDNA synthesis. Total RNA was extracted using the Total RNA Kit (E.Z.N.A®, Omega Bio-Tek, Norcross, GA, USA) according to the manufacturer's protocol. The concentration and purity of RNA were assessed by spectrophotometry, and RNA integrity was evaluated using the 260/280 absorbance ratio. A total of 500 ng of purified RNA was reverse-transcribed into complementary DNA (cDNA) using the High-Capacity cDNA Reverse Transcription Kit (Thermo Fisher Scientific Inc., Waltham, MA, USA), following the manufacturer's instructions.

2.7. Primer design and quantitative PCR (qPCR)

Primers were designed based on *Equus caballus* gene sequences obtained from the National Center for Biotechnology Information (NCBI), using the AmplifX software v2.0 (INRAE, Marceille, France). Quantitative PCR was then performed using gene-specific primers (Table 1) and the Brilliant II SYBR® Green QPCR Master Mix (Agilent Technologies, Santa Clara, CA, USA). For normalization, the ACTB gene was used as the reference gene. Reactions were run under standard cycling conditions recommended by the manufacturer. All reactions were carried out in triplicate, and appropriate no-template controls were included to verify the absence of contamination. Relative abundance of mRNA transcripts were calculated using the comparative $\Delta\Delta Ct$ method.

2.8. Statistical analysis

Each animal was treated as an experimental unit. To prevent pseudoreplication, repeated field and image measurements were averaged within animals before analysis. Assumptions were assessed on per-animal means using the Shapiro-Wilk test for normality and Levene's test for homogeneity of variances. Differences among Kenney-Doig grades (I, IIA, IIB) were evaluated using one-way ANOVA followed by Tukey's HSD; when assumptions were violated, Welch's ANOVA or Kruskal-Wallis with Dunn-Holm post hoc correction was applied.

Volume densities (Vv, %) were modeled as proportions using a logit transformation of Vv/100, with a small epsilon added for values of 0 or 100 %. When appropriate, a beta regression with grade as a fixed effect was preferred.

The relative abundance of gene transcripts was analyzed on ΔCq values (rather than fold changes), and false discovery rate across genes was controlled using the Benjamini-Hochberg procedure. All tests were two-sided with $\alpha = 0.05$. Effect sizes are reported with 95 % confidence intervals. Analyses were performed in R (v4.x) using the stats, car, emmeans, rstatix, and betareg packages.

Table 1

Primer sequences used for quantitative PCR (qPCR) amplification of selected mule endometrial genes, designed from *Equus caballus* reference sequences (NCBI RefSeq).

Gen	Forward	Reverse	Amplicon bp	NCBI RefSeq
ACTB	GTCCCCAGCATGAAGAT	GTCCCCAGCATGAAGAT	98	NM_001081838.1
IL1B	GCCCAAAACAGATGAAGGGCAG	AAAGTTGGTGGGAGATTGAAGC	92	NM_001082526.1
TNFA	GCCTCAGCCTCTTCCTTC	GGCTTGTCACTTGGGGTTC	97	NM_001081819.2
IL6	CCAAAGTCCTGGTCCAGATCC	GTGAATGCAGCTTAGCCAGC	97	NM_001082496.2
TGFB	GGATGGCTGTCCCTTGATG	GGAAATGGCTGTCCCTTGATG	91	NM_001081849.1

Primer sequences (forward and reverse), amplicon size (bp), and accession numbers are listed for each target gene. Genes: Beta-actin (ACTB), Interleukin 1 beta (IL1B), Tumor necrosis factor alpha (TNFA), Interleukin 6 (IL6), Transforming Growth factor beta (TGFB).

3. Results

3.1. Histometric characteristics of the mule endometrium

Table 2 and **Fig. 1** present the results for the main morphometric variables assessed in endometrial biopsies from mules. These include epithelial height, the thicknesses of the compact and spongy layers, endometrial gland diameter, gland wall thickness, and lymphatic vessel diameter.

The descriptive statistical analysis of the volume density of histological structures in the endometrium of mules is shown in **Table 3** and **Fig. 2**. The variables analysed include the volume density of the total endometrial space, epithelium, compact and spongy layers, lymphatic vessels, and glandular and cellular components within both the compact and spongy regions.

Attending the Kenney and Doig classification (1986) 8 mules were included in category I, 7 in category IIA and 7 in category IIB. However, no mules were included in category III. Histometric characteristics of each Kenney and Doig characteristics was analyzed. Although slight numerical variations were observed between groups, most differences were not significant ($p < 0.05$), except for the glandular area, where group IIB showed a significant reduction ($p < 0.05$) (**Table 4**).

On the other hand, the density volume of the basal endometrial epithelium was $3.48 \pm 1.64\%$ in Type I, with a significant increase to $4.57 \pm 1.46\%$ in IIA, and a significant decrease $3.51 \pm 1.61\%$ in IIB, in the IIB group ($p < 0.05$). In the compact layer there was no variation between I and IIA, $12.06 \pm 3.89\%$ (I), $12.55 \pm 1.88\%$ (IIA), and a significant decrease in the group IIB, $9.84 \pm 1.95\%$ (IIB) ($p < 0.05$). The spongy layer showed proportions of $84.46 \pm 4.02\%$ (I), $83.75 \pm 3.36\%$ (IIA), and $86.80 \pm 2.88\%$ (IIB), with a higher density in IIB. The proportion of lymphatic vessels in the endometrial tissue was $3.72 \pm 3.04\%$ in Type I, $1.54 \pm 0.85\%$ in IIA, and $2.21 \pm 1.24\%$ in IIB, with the lowest expression in IIA ($p < 0.05$). Glands in the compact layer were more abundant in group IIA ($9.62 \pm 2.12\%$) than in group I ($9.08 \pm 3.47\%$), and group IIB ($8.16 \pm 2.15\%$), and glands in the spongy layer increased from $57.43 \pm 5.71\%$ (I) to $59.64 \pm 4.60\%$ (IIA) and $59.92 \pm 5.66\%$ (IIB), with no statistical differences observed ($p > 0.05$). As for the cells in the compact layer, a decrease was observed in IIB ($5.04 \pm 1.47\%$) compared to I ($5.17 \pm 1.88\%$) and IIA ($5.38 \pm 1.08\%$), and the cells in the spongy layer showed decreasing values from $25.19 \pm 6.61\%$ (I) to $21.78 \pm 3.02\%$ (IIA) and $17.36 \pm 2.43\%$ (IIB) ($p < 0.05$). The significant differences between groups for the variables analysed indicate progressive remodelling of the endometrium in mules with characteristics similar to those observed in mares with different degrees of degenerative endometrial fibrosis ($p < 0.05$) (**Table 5**).

3.2. Abundance of proinflammatory mRNA transcripts in the mule endometrium

A significant increase in the relative abundance of IL-1 β and IL-6 mRNA transcripts was observed in group IIA and IIB compared to Type I ($p < 0.05$), with higher levels of IL-1 β in IIA and IL-6 in IIB, suggesting a progressive activation of proinflammatory cytokines with the advancement of degenerative endometrial fibrosis. Likewise, TGF- β (a mediator associated with fibrosis and stromal remodelling) showed the highest relative abundance in group IIB, being significantly higher compared to the other groups. TNF- α showed a similar pattern, with a marked increase in group IIB compared to groups I and IIA, although there were no differences between the latter two ($p > 0.05$) (**Fig. 3**).

4. Discussion

The present study aimed to explore the structural organization of the mule endometrium using detailed histological and stereological molecular analyses. These findings provide a novel reference framework for understanding reproductive physiology in hybrid equids and for comparing their uterine features with those of mares and jennies.

Morphometric analysis confirmed a structural hierarchy of the endometrium (stratum spongiosum > stratum compactum > surface epithelium), consistent with the canonical organization described for equine uteri and with the functional predominance of the spongiosum during phases favoring uterine receptivity (Camozzato et al., 2019; Schöniger and Schoon, 2020). In our mule biopsies, the surface epithelium averaged $17.96 \mu\text{m}$ (range, 6.81 – $36.75 \mu\text{m}$), which falls within the magnitudes reported for mares during estrus in histomorphometric series (Herrera et al., 2018) and within broader epithelial ranges documented in postpartum mares (Katila, 1988). The compact layer averaged $43.98 \mu\text{m}$ (SD $23.84 \mu\text{m}$), in line with cycle-dependent modulation of stromal/epithelial compartments in mares (Camozzato et al., 2019; Morris et al., 2020). The spongiosum showed the greatest height (mean $733.73 \mu\text{m}$; SD

Table 2

Descriptive statistical values (mean \pm standard deviation [SD], range, and 25th and 75th percentiles) of the histometric characteristics of the mule endometrium; $n = 550$ observations (25 measurements/22 mules).

Variable	(Mean \pm SD) (μm)	Range (μm)	25th Percentile (μm)	75th Percentile (μm)
Epithelial height	17.96 ± 6.86	6.81 – 36.75	12.20	22.52
Compact layer thickness	43.98 ± 23.84	11.12 – 196.18	27.04	55.07
Spongy layer thickness	733.73 ± 197.31	237.62 – 1188.73	590.99	894.16
Gland diameter	33.71 ± 17.92	14.23 – 402.32	26.83	38.62
Gland wall thickness	6.17 ± 1.08	3.43 – 10.19	5.42	6.91
Lymphatic vessel diameter	25.00 ± 14.36	4.99 – 113.03	14.64	32.14

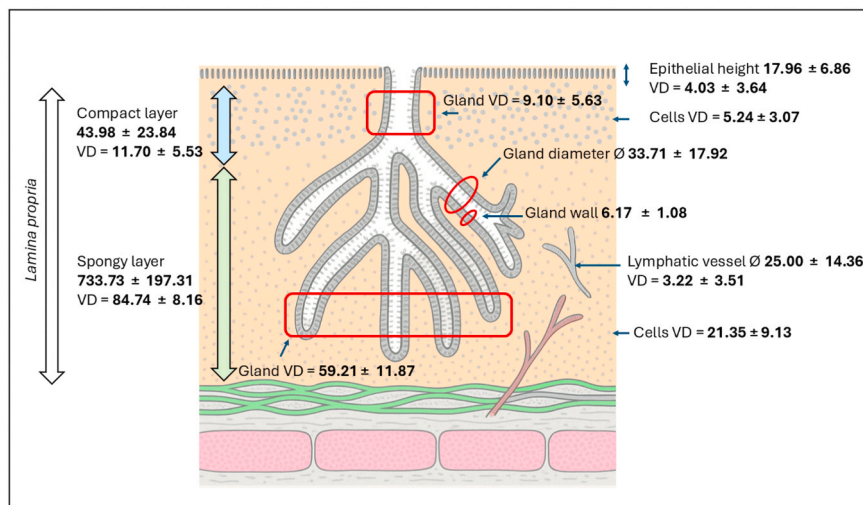


Fig. 1. Histological diagram of the mule endometrium, highlighting structural layers and key morphometric parameters. The compact and spongy layers of the lamina propria are depicted, along with endometrial glands, lymphatic vessels, and epithelial surfaces. Volume density (VD) values are expressed as percentages relative to the total volume of the endometrial biopsy, as estimated by unbiased stereology. All linear measurements are in micrometers (μm). Variability is reported as standard deviation ($\pm \text{SD}$).

Table 3

Descriptive statistical values (mean \pm standard deviation [SD], range, and 25th, 50th, and 75th percentiles) for volume density (VD) measurements of various histological structures within the endometrium of mules; $n = 1056$ points of study (48/22 mules).

Variable	Replicates per sample	(Mean \pm SD)	Range	25 %	50 %	75 %
Total Endometrium VD	110.00	100.0 \pm 0.00	100.00 – 100.00	100.00	100.00	100.00
Epithelial VD	110.00	4.03 \pm 3.64	0.03 – 17.65	0.01	3.71	5.88
Compact VD	110.00	11.70 \pm 5.53	0.01 – 35.29	8.00	10.71	14.29
Spongy VD	110.00	84.74 \pm 8.16	58.82 – 129.17	80.00	85.71	89.29
Lymphatic vessels VD	110.00	2.22 \pm 3.51	0.01 – 25.81	0.01	0.01	3.67
Compact glands VD	110.00	9.10 \pm 5.63	0.01 – 32.01	5.76	8.33	11.94
Spongy glands VD	110.00	59.21 \pm 11.87	28.02 – 86.21	50.00	59.26	66.67
Compact cells VD	110.00	5.24 \pm 3.07	0.01 – 16.01	3.45	5.01	6.91
Spongy cells VD	110.00	21.35 \pm 9.13	7.41 – 60.23	15.00	20.00	24.14

Values are expressed as percentages (%) relative to the total endometrial volume.

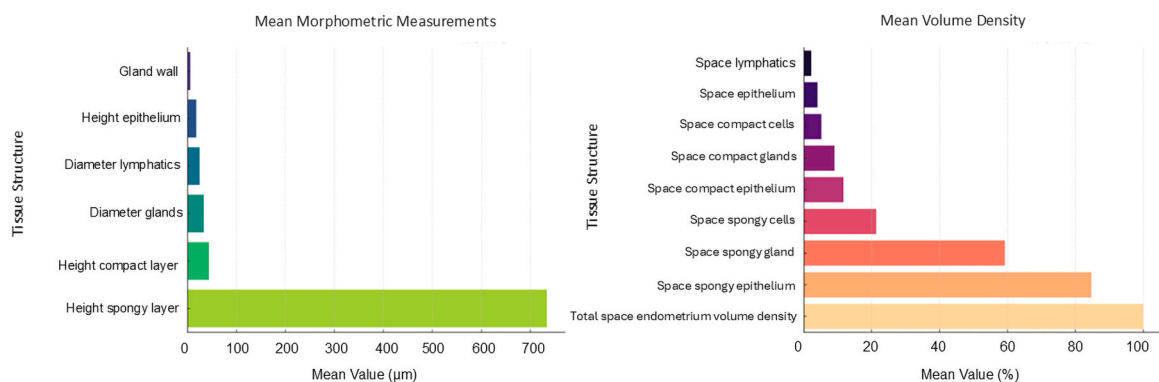


Fig. 2. Mean morphometric and volume density of mule endometrial components. Average height values (μm) of the three main structural layers of the mule endometrium: superficial epithelium, compact layer, and spongy layer, as well as the glandular diameter, glandular wall diameter, and lymphatic vessels.

197.31 μm), compatible with the well-known cyclic expansion of stromal/glandular components around the peri-luteal window (Camozzato et al., 2019; Caballeros et al., 2019).

For jennies, current high-quality studies emphasize species-specific histopathological and immunological traits (e.g., collagen

Table 4

Morphometric comparison of mule endometrium by kenney and doig.

Variable	Kenney and Doig			
	I (n = 8) (Mean ± SD)	IIA (n = 7) (Mean ± SD)	IIB (n = 7) (Mean ± SD)	III (Mean ± SD)
Epithelial layer height (μm)	28.51 ± 3.23 ^a	27.91 ± 3.10 ^a	26.70 ± 2.86 ^a	_____
Compact layer height (μm)	55.13 ± 4.51 ^a	52.82 ± 5.06 ^a	51.31 ± 4.93 ^a	_____
Spongy layer height (μm)	89.21 ± 6.36 ^a	87.54 ± 6.84 ^a	85.43 ± 7.22 ^a	_____
Total endometrial height (μm)	172.86 ± 9.58 ^a	168.21 ± 10.26 ^a	163.47 ± 11.16 ^a	_____
Gland diameter (μm)	34.72 ± 2.71 ^a	33.65 ± 3.11 ^a	31.91 ± 3.24 ^a	_____
Gland area (μm ²)	922.11 ± 100.46 ^a	899.47 ± 95.62 ^a	837.33 ± 92.51 ^b	_____
Number of glands per field	12.34 ± 1.21 ^a	11.81 ± 1.31 ^a	11.20 ± 1.46 ^a	_____
Lumen diameter (μm)	15.96 ± 1.43 ^a	15.12 ± 1.57 ^a	14.71 ± 1.68 ^a	_____
Lumen area (μm ²)	201.22 ± 30.36 ^a	198.78 ± 28.92 ^a	190.60 ± 27.53 ^a	_____

Values represent the mean ± standard deviation (SD) for each histological group. Group I corresponds to endometria without pathological changes; Groups IIA and IIB represent mild and moderate histological changes, respectively; and Group III (severe periglandular fibrosis and glandular degeneration) was not present. Different superscript letters (a) indicate statistically significant differences ($p < 0.05$).

Table 5

Percentage of endometrial structure density volume in mules according to Kenney and Doig classification.

Kenney and Doig classification	Epithelial (%)	Compact Epithelial (%)	Spongiosus Epithelial (%)	Lymphatic Vessels (%)	Compact Glands (%)	Spongiosus Glands (%)	Compact Cells (%)	Spongiosus Cells (%)
I (n = 8)	3.48 ± 1.64 ^a	12.06 ± 3.89 ^a	84.46 ± 4.02 ^a	3.72 ± 3.04 ^a	9.08 ± 3.47 ^a	57.43 ± 5.71 ^a	5.17 ± 1.88 ^a	25.19 ± 6.61 ^a
IIA (n = 7)	4.57 ± 1.46 ^b	12.55 ± 1.88 ^a	83.75 ± 3.36 ^a	1.54 ± 0.85 ^b	9.62 ± 2.12 ^a	59.64 ± 4.60 ^a	5.38 ± 1.08 ^a	21.78 ± 3.02 ^b
IIB (n = 7)	3.51 ± 1.61 ^a	9.84 ± 1.95 ^b	86.80 ± 2.88 ^b	2.21 ± 1.24 ^c	8.16 ± 2.15 ^a	59.92 ± 5.66 ^a	5.04 ± 1.47 ^a	17.36 ± 2.43 ^c
III	-	-	-	-	-	-	-	-

Endometrial density volume (%); Kenney and Doig endometrium classification, I: normal endometrium; IIA: Acute inflammation; IIB: Moderate-chronic inflammation; III: Degenerative endometrial fibrosis values are shown as Mean ± standard deviation (%). Different letters within the same column indicate significant differences between Kenney and Doig classification groups ($p < 0.05$). Lowercase letters denote specific multiple comparisons between groups.

patterning and eosinophilic infiltration; resident T-cell predominance) rather than precise epithelial height benchmarks, supporting a shared horse–donkey endometrial physiology with distinct immuno-stromal nuances (Miró et al., 2020; Radar-Chafirovitch et al., 2025).

The stroma (surface epithelium 4.03 %, stratum compactum ≈11.7 %, and stratum spongiosum 84.74 %) accounted for the majority of endometrial volume in mules, a distribution consistent with the layered organization and functional dominance of the spongy stratum reported for the equine endometrium (Lefranc and Allen, 2007; Hanada et al., 2012; Schöniger and Schoon, 2020). This pattern aligns with quantitative studies in mares, which show high gland concentration and the functional relevance of the stratum spongiosum, as well as with morphologic reviews detailing the stromal–glandular interdependence during the cycle (Lefranc and Allen, 2007).

In donkeys, comparative pathology points to species-specific features (e.g., eosinophil-rich infiltrates and distinct collagen patterns) and to immune-cell distributions that differ from mares, supporting cautious inter-species comparisons (Miró et al., 2020). In our series, glandular density was clearly higher in the spongy than in the compact stratum (59.21 % vs. 9.10 %), in line with studies that localized greater glandular surface density within the stratum spongiosum of mares. Lymphatic structures showed low but heterogeneous volume fractions (2.22 %, SD 3.51 %); while direct morphometric diameter benchmarks in equids are scarce, functional and lesion-oriented evidence indicates that uterine lymphatics contribute to clearance and may form lacunae in degenerative settings (LeBlanc et al., 1995). Finally, glandular dimensions in mules (diameter 33.71 ± 17.92 μm; wall 6.17 ± 1.08 μm) fall within ranges reported by quantitative histology in mares, supporting preservation of a secretory architecture compatible with a physiologically active endometrium (Herrera et al., 2018).

Mule endometrial biopsies, classified according to the Kenney and Doig system (Grades I, IIA, IIB), predominantly exhibited mild to moderate, organized tissue remodeling, consistent with early stages of degenerative endometrial fibrosis but without evidence of architectural collapse. This reading is consistent with the histopathological definition and prognostic scope of the Kenney–Doig system and its updates in mares (Westendorf et al., 2021). This structural stability may reflect the unique reproductive physiology of hybrids, characterized by limited gonadal function and the absence of regular estrous cycles, which likely reduces exposure to cyclical hormonal fluctuations. It should be noted: many female mules are acyclic or show irregular cyclicity, but there are also reports of cyclical mules and pregnancies after embryo transfer; therefore, the lower "average" exposure to complete cycles is plausible but not universal (Camillo et al., 2003). Previous studies in equines have suggested a lower susceptibility to progressive fibrosis under certain

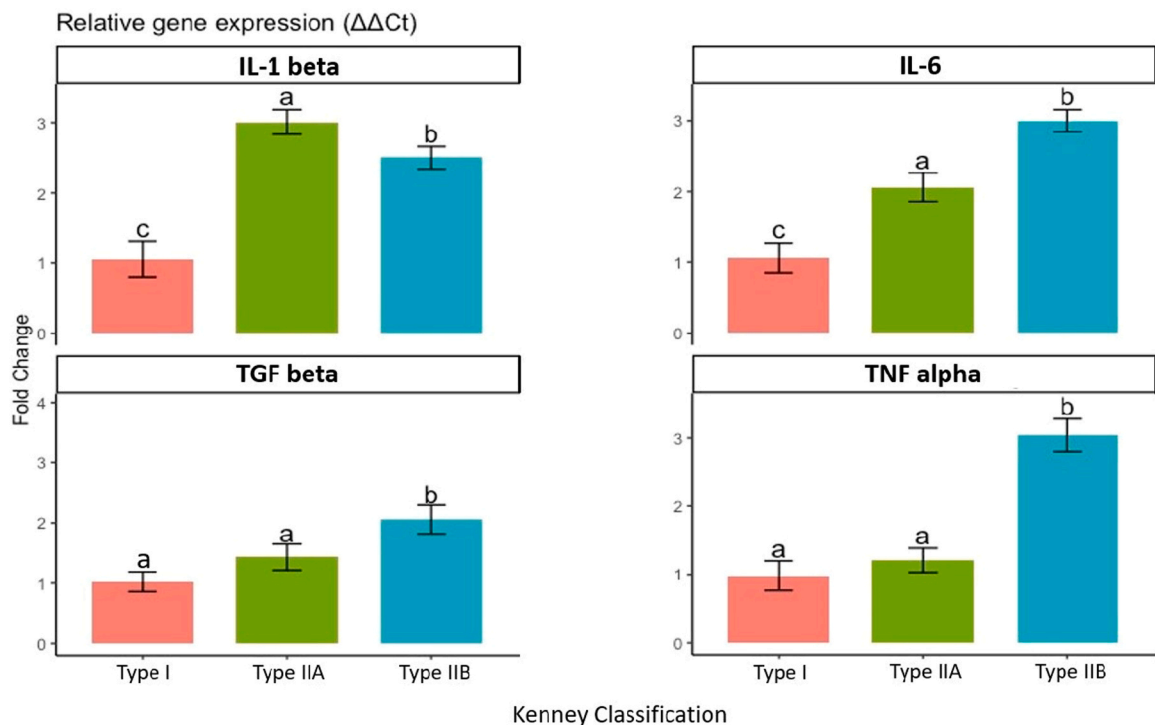


Fig. 3. Relative abundance of mRNA of proinflammatory gene transcripts in the mule endometrium classified according to Kenney and Doig classification (Types I, IIA, and IIB). Type III was not represented in the samples analysed. The genes analysed by real-time PCR were IL-1 β , IL-6, TGF- β , and TNF- α . Results are shown as relative fold change ($\Delta\Delta Ct$) compared to the Type I group. Bars indicate the Standard Deviation of the Mean (SD). Different letters above the columns indicate significant differences between groups ($p < 0.05$).

physiological conditions (Katila and Ferreira-Dias, 2022).

The age of the mules included in the study may also have influenced the results obtained. The study used mules aged between five and ten years, but no aged animals were included. The association between endometriosis severity (including category III) and age/infertility/repeated reproductive stimuli is well documented in mares, supporting the idea that progression can be attenuated with lower cumulative exposure (Lehmann et al., 2011). However, given the sterility, age range, and genetic heterogeneity of mules, these observations warrant further validation through direct comparisons with data from mares and donkeys. On the other hand, as explained before, preliminary evidence indicates that the mule endometrial structure may resemble that of the donkey more than that of the mare (Canisso et al., 2019). The donkey endometrium also appears to progress more slowly toward fibrosis and to maintain fertility into more advanced ages (Miró et al., 2020). Recent literature specifically underscores the need for comparative and donkey- and mule-specific frameworks (uterine physiology and immunology), supporting the call for direct cross-species validation.

In contrast, the mule uterus is functional as a gestational recipient for embryo transfer (Davies et al., 1985), consistent with a non-terminal remodeling profile. The uterine function of the mule as a recipient has been demonstrated with equine embryos and also with donkey embryos in non-cycling hormonally treated mules. Furthermore, hybrid immune phenotypes could modulate chronic inflammation/fibrosis (Ferreira-Dias et al., 2024). In equines, recent reviews report that immune pathways (e.g., NF- κ B; proinflammatory cytokines) modulate endometrial fibrosis. In donkeys, the endometrial immune population has been mapped, supporting species-specific differences that could be transferred to hybrids. We propose considering an IIC subcategory within IIB to describe moderate fibrous remodeling without collapse. The lack of marked changes even in IIB and the increase in glands in the spongy layer, along with reductions in the stratum compactum, lymphatics, spongy layer, and epithelium, support this hypothesis.

Transcriptional profiling revealed immune activation at intermediate stages, with IL-1 β and IL-6 mRNA transcripts relative abundance increasing in grades IIA and IIB. This is consistent with the activation of these mediators during endometritis-induced inflammation in mares—with early increases in IL-1 β , IL-6, and TNF- α —and with transcriptional modulation depending on the type and chronicity of inflammation (Christoffersen et al., 2012). This pattern aligns with their pivotal role as mediators between physiological function and chronic inflammation/remodeling in mares, as summarized in mechanistic reviews on PBIE and the transition to degenerative processes (Morris et al., 2020), and with their reported overexpression during degenerative processes in donkeys. In jennets, direct evidence on IL-1 β /IL-6 is still limited. However, differential immunologic and histopathologic features (e.g., eosinophil infiltrates, collagen remodeling) and a resident immune cell landscape dominated by T lymphocytes, compatible with a sustained tissue inflammatory response, have been described (Miró et al., 2020). Relative abundance of TNF- α transcript was elevated in Grade IIB, a finding associated with decreased endometrial receptivity and glandular-stromal alterations previously described in mares (association between uterine inflammation, cytokines, and decreased receptivity/chronic endometrosis) (Morris et al., 2020).

The sustained increase in TGF- β in IIB is compatible with profibrotic remodeling and collagen deposition—TGF- β 1 induces myofibroblast differentiation and COL1/COL3 synthesis in equine endometrium; furthermore, TGF- β 1 has been correlated with endometrial fibrosis (Szóstek-Mioduchowska et al., 2019). The absence of Grade III in our cohort underscores a pathophysiological trajectory distinct from that observed in mares exposed to prolonged reproductive insults and is consistent with the classic progression described by Kenney-Doig/Schoon toward advanced fibrosis in older mares or mares with a prolonged reproductive history (Schöniger and Schoon, 2020), and suggests that, in mules, inflammation does not progress to terminal fibrosis. From a comparative physiology perspective, natural sterility and less exposure to full cycles could buffer the progression to terminal lesions (Schöniger and Schoon, 2020). Gestational viability after embryo transfer without placental dysfunction in mules has been documented in controlled studies and successful cases, supporting an intermediate but functional histomolecular phenotype (Camargo et al., 2020). Equine endometrial transcriptomics and recent embryo-endometrium interaction studies provide frameworks and methodologies to validate biomarkers (Weber et al., 2021) to assess the prognostic relevance of inflammatory (IL-6, IL-1 β , TGF- β 1, TNF- α) and fibrotic (COL1A1, COL3A1) markers. (functional tests of TGF- β 1 \rightarrow COL1/COL3 and profibrotic pathways in equine endometrium) (Szóstek-Mioduchowska et al., 2019). This approach could help refine diagnostic systems to better accommodate the unique physiology of hybrids. Prior studies in mares and donkeys (Rebordão et al., 2014; Centeno et al., 2024; Gambini et al., 2025) support the potential utility of these biomarkers in equine endometrial pathology. Applying the Kenney-Doig classification to mules offers a useful framework for prognostic assessment and clinical decision-making; However, its validation and potential adaptation require correlation between histopathological and molecular findings with current conception and gestation outcomes in this hybrid species. (Kenney-Doig reliability and variability; need to validate against outcomes) (Westendorf et al., 2021).

Collectively, these data provide a robust anatomical reference to define physiological standards relevant to infertility work-ups, hormonal therapies, and embryo-transfer protocols across equids (Schöniger and Schoon, 2020).

5. Conclusions

This study presents the first quantitative morphometric and molecular characterization of the mule endometrium, revealing a distinct, intermediate phenotype that leans toward asinine features while retaining equine traits. Several structural metrics align with values reported in both mares and jennies, underscoring the hybrid's unique uterine architecture. We identified consistent histomorphometric patterns and mRNA transcriptional profiles indicative of mild to moderate degenerative endometrial fibrosis, supporting the value of integrating histological and molecular assessments in the reproductive evaluation of mules. Our findings suggest that the Kenney-Doig classification system, originally developed for mares, can be adapted for hybrid use (with a proposed refinement of the IIC category) to better reflect hybrid-specific endometrial changes. Altogether, this work establishes a foundational framework for future studies on mule reproductive physiology and positions the mule as a valuable comparative model in equine reproductive pathology and hybrid reproductive management.

CRediT authorship contribution statement

Daniela Rojas: Methodology, Investigation. **Yat Sen Wong:** Investigation, Data curation. **Fernando Saravia:** Resources, Methodology, Funding acquisition. **Fidel Ovidio Castro:** Resources, Methodology, Data curation. **Jaime Catalán:** Writing – review & editing, Supervision, Resources. **Miro Jordi:** Writing – review & editing, Supervision, Resources, Conceptualization. **Miguel A. Gutiérrez-Reinoso:** Writing – original draft, Project administration, Methodology, Investigation, Funding acquisition, Formal analysis, Data curation. **Pedro M. Aponte:** Methodology, Investigation, Conceptualization. **Manuel García-Herreros:** Investigation. **Katlien G. García-Bravo:** Methodology, Investigation.

Institutional Review Board Statement

The authors declare that this study was conducted in strict accordance with ethical principles for animal research, following the international ARRIVE guidelines (Animal Research: Reporting of In Vivo Experiments), available at <http://www.nc3rs.org.uk/ARRIVEchecklist> (accessed July 7, 2023). The experimental protocol was reviewed and approved by the Bioethics Committee for the Use of Experimental Animals at the Universidad de Concepción, Chillán Campus, Chile, under approval number CBE-8269/2023, dated September 1, 2023.

Funding sources

This research was partially funded by the Equine Reproduction Service, Universitat Autònoma Barcelona (Spain), DIRGI-CP2021-005/Universidad Técnica de Cotopaxi (Ecuador), Instituto de Investigaciones en Biomedicina "One-Health", Universidad San Francisco de Quito (Ecuador), y el Department of Animal Science, Faculty of Veterinary Sciences, Universidad de Concepción (Chile). J.C. was funded by the Ministry of Science, Innovation and Universities, Spain (MCIN/AEI/10.13039/501100011033) and the European Union NextGenerationEU/PRTR (Juan de la Cierva Scheme: JDC2022-049684-I).

Declaration of Competing Interest

The authors of the manuscript entitled "Histomorphometric Characterization of the Endometrium in Mules (*Equus mulus*): an

approach to endometritis/endometriosis" declare that they have no conflicts of interest.

Acknowledgments

We would like to acknowledge the efforts of all individuals and laboratories involved in the execution of this research.

Data Availability

Raw data supporting the findings of this study are available from the corresponding author on request.

References

Adavoudi, R., Pilot, M., 2022. Consequences of hybridization in mammals: a systematic review. *Genes* 13, 50. <https://doi.org/10.3390/genes13010050>.

Allen, W.R., 2005. The development and application of the modern reproductive technologies to horse breeding. *Reprod. Domest. Anim.* 40, 310–329. <https://doi.org/10.1111/J.1439-0531.2005.00602.X>.

Allen, W.R., Short, R.V., 1997. Interspecific and extraspecific pregnancies in equids: anything goes. *J. Hered.* 88, 384–392. <https://doi.org/10.1093/oxfordjournals.jhered.a023123>.

Bottrel, M., Fortes, T., Ortiz, I., Hidalgo, M., Dorado, J., 2017. Establishment and maintenance of donkey-in-mule pregnancy after embryo transfer in a non-cycling mule treated with oestradiol benzoate and long-acting progesterone. *Span. J. Agric. Res.* 15, e045C01. <https://doi.org/10.5424/sjar/2017154-11653>.

Caballeros, J.E., Camacho, C., Cazales, N., Estradé, M.J., Fiala-Rechsteiner, S., Jobim, M.I.M., Mattos, R.C., 2019. Ultrastructural and histological characteristics of the equine endometrium at day 5 post ovulation. *Theriogenology* 132, 106–112. <https://doi.org/10.1016/j.theriogenology.2019.04.006>.

Camargo, C.E., Rechsteiner, S.F., Macan, R.C., Kozicki, L.E., Gastal, M.O., Gastal, E.L., 2020. The mule (*Equus mulus*) as a recipient of horse (*Equus caballus*) embryos: comparative aspects of early pregnancy with mares: the mule as a recipient of horse embryos. *Theriogenology* 145, 217–225. <https://doi.org/10.1016/j.theriogenology.2019.10.029>.

Camillo, F., Vannozzi, I., Rota, A., Di Luzio, B., Romagnoli, S., Aria, G., Allen, W.R., 2003. Successful non-surgical transfer of horse embryos to mule recipients. *Reprod. Domest. Anim.* 38, 380–385. <https://doi.org/10.1046/J.1439-0531.2003.00444.X>.

Camozzato, G.C., Martinez, M.N., Bastos, H.B.A., Fiala-Rechsteiner, S., Meikle, A., Jobim, M.I.M., Gregory, R.M., Mattos, R.C., 2019. Ultrastructural and histological characteristics of the endometrium during early embryo development in mares. *Theriogenology* 123, 1–10. <https://doi.org/10.1016/j.theriogenology.2018.09.018>.

Canisso, I.F., Panzani, D., Miró, J., Ellerbrock, R.E., 2019. Key aspects of donkey and mule reproduction. *Vet. Clin. North Am. Equine Pr.* 35, 607–642. <https://doi.org/10.1016/j.cveq.2019.08.014>.

Centeno, L.A.M., Bastos, H.B.A., Bueno, V.L.C., Trentin, J.M., Fiorenza, M.F., Panziera, W., Winter, G.H.Z., Kretzmann, N.A., Fiala-Rechsteiner, S., Mattos, R.C., Rubin, M.I.B., 2024. Collagen and collagenases in mare's endometrium with endometrosis. *Theriogenology* 230, 28–36. <https://doi.org/10.1016/j.theriogenology.2024.08.031>.

Christoffersen, M., Woodward, E., Bojesen, A.M., Jacobsen, S., Petersen, M.R., Troedsson, M.H.T., Lehn-Jensen, H., 2012. Inflammatory responses to induced infectious endometritis in mares resistant or susceptible to persistent endometritis. *BMC Vet. Res.* 8, 41. <https://doi.org/10.1186/1746-6148-8-41>.

Davies, C.J., Antczak, D.F., Allen, W.R., 1985. Reproduction in mules: embryo transfer using sterile recipients. *Equine Vet. J.* 17, 63–67. <https://doi.org/10.1111/j.1365-2710.1985.tb04595.x>.

Davis, E., 2019. Donkey and mule welfare. *Vet. Clin. North Am. Equine Pr.* 35, 481–491. <https://doi.org/10.1016/j.cveq.2019.08.005>.

Elshalofy, A., Wagener, K., Weber, K., Blanco, M., Bauersachs, S., Bollwein, H., 2022. Identification of genes associated with susceptibility to persistent breeding-induced endometritis by RNA-sequencing of uterine cytobrush samples. *Reprod. Biol.* 22, 100577. <https://doi.org/10.1016/j.repbio.2021.100577>.

Fanelli, D., Losinno, L., Castañeira, C., Alonso, C., Bragulat, A., Panzani, D., Bocci, C., Degl'Innocenti, A., Moroni, R., Camillo, F., Wilsher, S., (Twink) Allen, W., 2022. First report of mule-in-mule pregnancies with live births following embryo transfer. *J. Equine Vet. Sci.* 113, 103999. <https://doi.org/10.1016/j.jevs.2022.103999>.

Ferreira-Dias, G.M., Alpoim-Moreira, J., Szóstek-Mioduchowska, A., Rebordão, M.R., Skarzynski, D.J., Ferreira-Dias, G.M., Alpoim-Moreira, J., Szóstek-Mioduchowska, A., Rebordão, M.R., Skarzynski, D.J., 2024. The path to fertility: current approaches to mare endometritis and endometrosis. *Anim. Reprod.* 21, e20240070. <https://doi.org/10.1590/1984-3143-AR2024-0070>.

Gábryš, J., Kij, B., Kochan, J., Bugno-Poniewierska, M., 2021. Interspecific hybrids of animals in nature, breeding and science - a review. *Ann. Anim. Sci.* 21, 403–415. <https://doi.org/10.2478/aoas-2020-0082>.

Gambini, A., Smith, J.M., Gurkin, R.J., Palacios, P.D., 2025. Current and emerging advanced techniques for breeding donkeys and mules. *Animals* 15, 990. <https://doi.org/10.3390/ani15070990>.

González, S.M., Gomes, R.G., Souza, A.K., Silva, C.B., Silva-Santos, K.C., Seneda, M.M., 2015. Evidences of regular estrous cycles in mules and successful use of these animals as recipients for donkey embryos. *J. Equine Vet. Sci.* 35, 869–872. <https://doi.org/10.1016/j.jevs.2015.07.010>.

Hanada, M., Maeda, Y., Oikawa, M.A., 2012. Equine endometrial gland density and endometrial thickness vary among sampling sites in thoroughbred mares. *J. Equine Sci.* 23, 35–40. <https://doi.org/10.1294/jes.23.35>.

Henry, M., Gastal, E.L., Pinheiro, L.E.L., Guimaraes, S.E.F., 1995. Mating pattern and chromosome analysis of a mule and her offspring. *Biol. Reprod.* 52, 273–279. https://doi.org/10.1093/biolreprod/52.monograph_series1.273.

Herrera, M., Herrera, J.M., Cantatore, S., Aguirre, J., Felipe, A., Fumuso, E., 2018. Comparative histomorphological study of endometrium in mares. *Anat. Histol. Embryol.* 47, 153–158. <https://doi.org/10.1111/ahe.12335>.

Katila, T., 1988. Histology of the post partum equine uterus as determined by endometrial biopsies. *Acta Vet. Scand.* 29, 173–180. <https://doi.org/10.1186/BF03548368>.

Katila, T., Ferreira-Dias, G., 2022. Evolution of the concepts of endometrosis, post breeding endometritis, and susceptibility of mares. *Animals* 12, 779. <https://doi.org/10.3390/ani12060779>.

Kenney, R.M., Doig, P.A., 1986. Equine endometrial biopsy. In: Morrow, D.A. (Ed.), *Current Therapy in Theriogenology*. W.B. Saunders Co, Philadelphia, pp. 723–729.

Klein, C., 2015. Pregnancy Recognition and Implantation of the Conceptus in the Mare. *Adv. Anat. Embryol. Cell. Biol.* 216, 165–188. https://doi.org/10.1007/978-3-319-15856-3_9.

LeBlanc, M.M., Johnson, R.D., Calderwood Mays, M.B., Valderrama, C., 1995. Lymphatic clearance of india ink in reproductively normal mares and mares susceptible to endometritis. *Biol. Reprod.* 52, 501–506. https://doi.org/10.1093/biolreprod/52.monograph_series1.501.

Lection, J., Wagner, B., Byron, M., Miller, A., Rollins, A., Cheneir, T., Cheong, S.H., Diel de Amorim, M., 2024. Inflammatory markers for differentiation of endometritis in the mare. *Equine Vet. J.* 56, 678–687. <https://doi.org/10.1111/evj.14058>.

Lefranc, A.C., Allen, W.R., 2007. Influence of breed and oestrous cycle on endometrial gland surface density in the mare. *Equine Vet. J.* 39, 506–510. <https://doi.org/10.2746/042516407X235812>.

Lehmann, J., Ellerberger, C., Hoffmann, C., Bazer, F.W., Klug, J., Allen, W.R., Sieme, H., Schoon, H.A., 2011. Morpho-functional studies regarding the fertility prognosis of mares suffering from equine endometrosis. *Theriogenology* 76, 1326–1336. <https://doi.org/10.1016/j.theriogenology.2011.06.001>.

Miró, J., Gutiérrez-Reinoso, M., Silva, J.A., da, Fernandes, C., Rebordão, M.R., Alexandre-Pires, G., Catalán, J., Ferreira-Dias, G., 2020. Collagen and eosinophils in Jenny's endometrium: do they differ with endometrial classification. *Front. Vet. Sci.* 7, 558096. <https://doi.org/10.3389/fvets.2020.00631>.

Morris, L.H.A., McCue, P.M., Aurich, C., 2020. Equine endometritis: a review of challenges and new approaches. *Reproduction* 160, R95–R110. <https://doi.org/10.1530/REP-19-0478>.

Radar-Chafirovitch, A., Quaresma, M., Yáñez-Ortiz, I., Leiva, B., Ferreira-Dias, G., Payan-Carreira, R., Miro, J., Pires, M. dos A., 2025. Donkey endometrium: characterization of resident immune cells. *Res. Vet. Sci.* 184, 105516. <https://doi.org/10.1016/j.rvsc.2024.105516>.

Rebordão, M.R., Galvão, A., Szóstek, A., Amaral, A., Mateus, L., Skarzynski, D.J., Ferreira-Dias, G., 2014. Physiopathologic mechanisms involved in mare endometrosis. *Reprod. Domest. Anim.* 49, 82–87. <https://doi.org/10.1111/rda.12397>.

Rong, R., Chandley, A.C., Song, J., McBeath, S., Tan, P.P., Bai, Q., Speed, R.M., 1988. A fertile mule and hinny in China. *Cytogenet. Cell Genet.* 47, 134–139. <https://doi.org/10.1159/000132531>.

Rong, R.H., Cai, H.D., Yang, X.Q., Wei, J., 1985. Fertile mule in China and her unusual foal. *J. R. Soc. Med.* 78, 821–825. <https://doi.org/10.1177/014107688507801006>.

Runemark, A., Moore, E.C., Larson, E.L., 2024. Hybridization and gene expression: Beyond differentially expressed genes. *Mol. Ecol.* 34, e17303. <https://doi.org/10.1111/mec.17303>.

Ryder, O.A., Chemnick, L.G., Bowling, A.T., Benirschke, K., 1985. Male mule foal qualifies as the offspring of a female mule and jack donkey. *J. Hered.* 76, 379–381.

Schöniger, S., Schoon, H.A., 2020. The healthy and diseased equine endometrium: a review of morphological features and molecular analyses. *Animals* 10, 625. <https://doi.org/10.3390/ani10040625>.

Szóstek-Mioduchowska, A.Z., Baclawska, A., Okuda, K., Skarzynski, D.J., 2019. Effect of proinflammatory cytokines on endometrial collagen and metallopeptidase expression during the course of equine endometrosis. *Cytokine* 123, 154767. <https://doi.org/10.1016/j.cyto.2019.154767>.

Ulaangerel, T., Mu, S., Sodylealt, J., Yi, M., Zhao, B., Hao, A., Wen, X., Han, B., Bou, G., 2025. Transcriptome analysis reveals equine endometrium's gene expression profile around embryo fixation. *Genes* 16, 181. <https://doi.org/10.3390/genes16020181/S1>.

Weber, K.S., Wagener, K., Blanco, M., Bauersachs, S., Bollwein, H., 2021. A comparative analysis of the intrauterine transcriptome in fertile and subfertile mares using cytobrush sampling. *BMC Genom.* 22, 377. <https://doi.org/10.1186/S12864-021-07701-3>.

Westendorf, J., Wobeser, B., Epp, T., 2021. IIB or not IIB, part 1: retrospective evaluation of Kenney–Doig categorization of equine endometrial biopsies at a veterinary diagnostic laboratory and comparison with published reports. *J. Vet. Diagn. Invest.* 34, 206–214. <https://doi.org/10.1177/10406387211062207>.

Woodward, E.M., Troedsson, M.H.T., 2015. Inflammatory mechanisms of endometritis. *Equine Vet. J.* 47, 384–389. <https://doi.org/10.1111/evj.12403>.